NeuroImage: Clinical 20 (2018) 955–971

Contents lists available at ScienceDirect

NeuroImage: Clinical

journal homepage: www.elsevier.com/locate/ynicl

Lesion locations associated with persistent proprioceptive impairment in the upper limbs after stroke

Sonja E. Findlater[a], Rachel L. Hawe[a], Jennifer A. Semrau[a], Jeffrey M. Kenzie[a], Amy Y. Yu[b], Stephen H. Scott[c,d], Sean P. Dukelow[a,b,*]

[a] Division of Physical Medicine and Rehabilitation, Department of Clinical Neurosciences, Hotchkiss Brain Institute, Faculty of Kinesiology, University of Calgary, 2500 University Dr. NW, Calgary, AB T2N 1N4, Canada
[b] Calgary Stroke Program, Department of Clinical Neurosciences, Hotchkiss Brain Institute, University of Calgary, 2500 University Dr. NW, Calgary T2N 1N4, AB, Canada
[c] Department of Anatomy and Cell Biology, Queen's University, Botterell Hall, Room 219, Kingston, ON K7L 3N6, Canada
[d] Providence Care, St. Mary's of the Lake Hospital, 340 Union St, Kingston, ON, Canada, K7L 5A2

ARTICLE INFO

Keywords:
Proprioception
Lesion analysis
Stroke
Upper extremity
Robotic assessment

ABSTRACT

Proprioceptive deficits are common after stroke and have been associated with poorer recovery. Relatively little is known about the brain regions beyond primary somatosensory cortex that contribute to the percept of proprioception in humans. We examined a large sample (n = 153) of stroke survivors longitudinally to determine which brain regions were associated with persistent post-stroke proprioceptive deficits. A robotic exoskeleton quantified two components of proprioception, position sense and kinesthesia (movement sense), at 2 weeks and again at 6 months post-stroke. A statistical region of interest (sROI) analysis compared the lesion-behaviour relationships of those subjects with cortical and subcortical stroke (n = 136). The impact of damage to brainstem and cerebellum (n = 17) was examined separately. Results indicate that damage to the supramarginal gyrus, the arcuate fasciculus, and Heschl's gyrus are associated with deficits in position sense and kinesthesia at 6 months post-stroke. These results suggest that regions beyond the primary somatosensory cortex contribute to our sense of limb position and movement. This information extends our understanding of proprioceptive processing and may inform personalized interventions such as non-invasive brain stimulation where specific brain regions can be targeted to potentially improve stroke recovery.

1. Introduction

Proprioception is a term originally coined by Sherrington (1907). It represents our sense of limb position and movement. Position sense and kinesthesia (movement sense) appear to originate in the periphery via differential signals derived largely from muscle spindles (McCloskey, 1973). Afferent proprioceptive information travels to the brain via the spinal cord in two systems. The dorsal-column medial lemniscal tract ascends the dorsal columns, synapses and crosses the midline in the medulla, ascends to synapse at the ventral posterior lateral nucleus of the thalamus, and, finally projects to the cortical somatosensory regions (Felton and Shetty, 2010; Pearson and Gordon, 2013; Purves et al., 2008). Secondly, proprioceptive information destined for the cerebellum ascends the spinal cord via the posterior spinocerebellar (lower limbs) and cuneocerebellar (upper limbs) tracts and enters the spinocerebellum via the ipsilateral cerebellar peduncle (Lisberger and Thach, 2012; Oscarsson and Uddenberg, 1964). Proprioceptive information at the cerebellar level is used to adjust posture and on-line movement (Pearson and Gordon, 2013) while higher level processing of proprioceptive information occurs in cortical areas like the parietal cortex (Amaral, 2013; Gardner and Johnson, 2013). While a few functional imaging studies (Ben-Shabat et al., 2015; Naito et al., 2017; Naito et al., 2007; Naito et al., 2005; Weiller et al., 1996) have examined the central aspects of proprioception in the brain in healthy humans, there is still much to learn. Stroke leads to discrete lesions in the brain and thus creates an interesting model to determine brain regions that are important for our sense of limb position and movement by comparing lesion location with behavioural impairment.

Stroke is a common central neurologic condition that can damage areas of the brain involved in proprioception. Impairments in proprioception occur in up to 64% of individuals after stroke (Connell et al., 2008). These impairments are associated with poor functional recovery and decreased independence (Carey and Matyas, 2011) as well as disturbed motor learning (Vidoni and Boyd, 2009). To date, however, few

* Corresponding author at: 1403 29th St NW, South Tower – Room 905, Calgary, Alberta, T2N 2T9 Canada.
E-mail address: spdukelo@ucalgary.ca (S.P. Dukelow).

https://doi.org/10.1016/j.nicl.2018.10.003
Received 27 August 2018; Received in revised form 1 October 2018; Accepted 3 October 2018
Available online 04 October 2018

longitudinal studies have investigated proprioceptive recovery after stroke. Connell et al. (2008) followed 70 stroke subjects for the first 6 months post stroke and reported that despite high inter-individual variability, upper extremity proprioception for the group significantly improved over time. Meyer et al. (2016a) followed 32 subjects out to 6 months post stroke and found proprioceptive recovery was highly variable depending on which clinical measure was used. Both studies relied on clinical tests of proprioception, which have known challenges with accuracy, precision and reliability (Lincoln et al., 1991). To overcome some of these challenges, our group has recently used a robotic exoskeleton to examine proprioceptive and motor recovery in a large longitudinal sample and found that recovery was highly variable between individuals (Semrau et al., 2015). Interestingly, we observed differential recovery of position sense and kinesthesia, two subcomponents of proprioception.

We have previously examined brain regions associated with impaired position sense and kinesthesia in the first two weeks post-stroke. Impaired arm position sense was associated with damage to the posterior parietal cortex, the transverse temporal gyrus (Heschl's gyrus), and the arcuate fasciculus (Findlater et al., 2016). Impaired kinesthesia was associated with lesions in the postcentral gyrus, the supramarginal gyrus, the insula, superior temporal gyrus, and the parietal operculum (Kenzie et al., 2016). Another group recently assessed proprioception using the Erasmus MC modification of the (revised) Nottingham sensory assessment (Lincoln et al., 1998). At one-week post-stroke proprioceptive deficits were associated with damage to the parietal operculum, superior thalamic radiation, insulo-opercular cortex, and the corticospinal tract (Meyer et al., 2016b). However, whether these regions predict proprioceptive deficits that persist into the chronic stage post-stroke is an open question given the potential for diaschesis and brain reorganization in the weeks and months following stroke.

Other groups studying different post-stroke impairments have found that lesion/behaviour associations observed initially post-stroke may not hold true in the chronic stage. Perhaps this is not surprising giving that substantial neuroplasticity can occur over the first several months post-stroke. Examples include a longitudinal neglect study by Karnath et al. (2011) that reported a number of lesion locations associated with acute neglect that were not associated with persistent neglect. Similarly, functional MRI analyses investigating motor function observed that regional connectivity changed over time (Ovadia-Caro et al., 2013). Finally, diffusion tractography studies have demonstrated structural reorganization overtime (Doughty et al., 2016; Puig et al., 2010; Thomalla et al., 2005). Together, these findings caution that lesion/behaviour relationships change over time, highlighting the importance of completing lesion/behaviour analyses that relate to the time point of interest.

Given that little is known about brain regions associated with persistent proprioceptive deficits following stroke, the present study aimed to determine the lesion locations associated with these issues. First, we examined cortical and subcortical lesions and hypothesized that the regions associated with persistent position sense and kinesthetic deficits would differ somewhat from those at 2 weeks post-stroke. Further, we hypothesized that cortical and subcortical lesion locations associated with persistent position sense deficits would differ from regions associated with kinesthetic deficits. Finally, we examined the impact of brainstem and cerebellar stroke lesions on proprioception since little has been reported about proprioceptive recovery in these types of lesions.

2. Materials and methods

2.1. Participants

We included subjects with first-time unilateral stroke who were able to follow the instructions required to complete the robotic and clinical assessments. Subjects were excluded if they had upper extremity pain, orthopedic injuries to the upper extremity, pre-existing neurological conditions (e.g. Multiple Sclerosis, Parkinson's Disease), apraxia (Cassidy, 2016; van Heugten et al., 1999), or a poorly defined lesion on neuroimaging. All subjects with stroke (n = 153) had clinical imaging collected within 10 days of stroke onset.

Control subjects were recruited from the community via recruitment posters and word of mouth. A member of the study team screened potential control subjects to rule out any neurological or orthopedic conditions that would impede their ability to complete the robotic and clinical assessments.

All subjects provided written informed consent to participate in this study in accordance with the Declaration of Helsinki. The University of Calgary Conjoint Health Research Ethics Board approved this study.

2.2. Robotic assessment

Robotic measures of proprioception and visuomotor abilities were conducted for all subjects with stroke at approximately 2 and 26 weeks post-stroke.

2.2.1. Device

Robotic assessments were conducted using two proprioceptive tasks and a visually guided reaching task with a KINARM exoskeleton robot (BKIN Technologies Ltd., Kingston, Ontario). Subjects were seated comfortably on the wheelchair base and the study therapist adjusted the exoskeleton to each subjects' height and limb geometry. Forearm and arm troughs supported each arm, permitting free, near-frictionless movement in the horizontal plane.

2.2.2. Assessment of position sense

The first task, position matching, assessed the individual's sense of the position of their arm and has been described previously (Dukelow et al., 2012; Dukelow et al., 2010; Herter, 2011; Semrau et al., 2013a, 2013b) (Fig. 1A). In this task, the subject's vision of their arms was occluded. The robot moved one arm (*passive arm*) in a pseudo-random order to one of 9 spatial locations. The subject then mirror-matched this position with their opposite, *active,* arm. Subjects notified the examiner when they had completed the match and the examiner then triggered the next trial. Six blocks of the 9 spatial locations were completed for a total of 54 trials. In participants with stroke the affected arm was only ever used as the *passive arm*. Controls completed the task twice with each arm serving as the *passive arm* once.

Three patterns of spatial errors (parameters) were quantified with the position matching task. All parameters have been previously described (Dukelow et al., 2010). Briefly, the *variability* parameter measured the trial-to-trial variability of the matching hand (Fig. 1B). It was calculated as the standard deviation of the matched x, y target location for each target, and then averaged across all 9 targets. The *contraction/expansion* parameter describes the subjects' perceived workspace area (Fig. 1C). The area subtended by the subject to match the outer targets was divided by the area of the square made by the robot's target locations. The *spatial shift* parameter measures the perception of workspace location (Fig. 1D). The mean error between the matching hand and the robotically-moved hand for each target location was calculated to determine if the subject perceived a shift in the x, y, or xy directions of the workspace. Finally, an overall *task score* was calculated to indicate overall performance on the position sense task. Task score calculation details are located in Section 2.2.5.

2.2.3. Assessment of kinesthesia

The kinesthetic matching task assessed the sense of arm motion and has been described previously (Kenzie et al., 2017; Semrau et al., 2017; Semrau et al., 2013a, 2013b; Semrau et al., 2015) (Fig. 1E). In this task, subjects' vision of their arms was occluded. Before the start of each trial, the robot moved the *passive arm* to one of three locations. At the same time, subjects saw a red circle on the workspace (located at 1 of 3

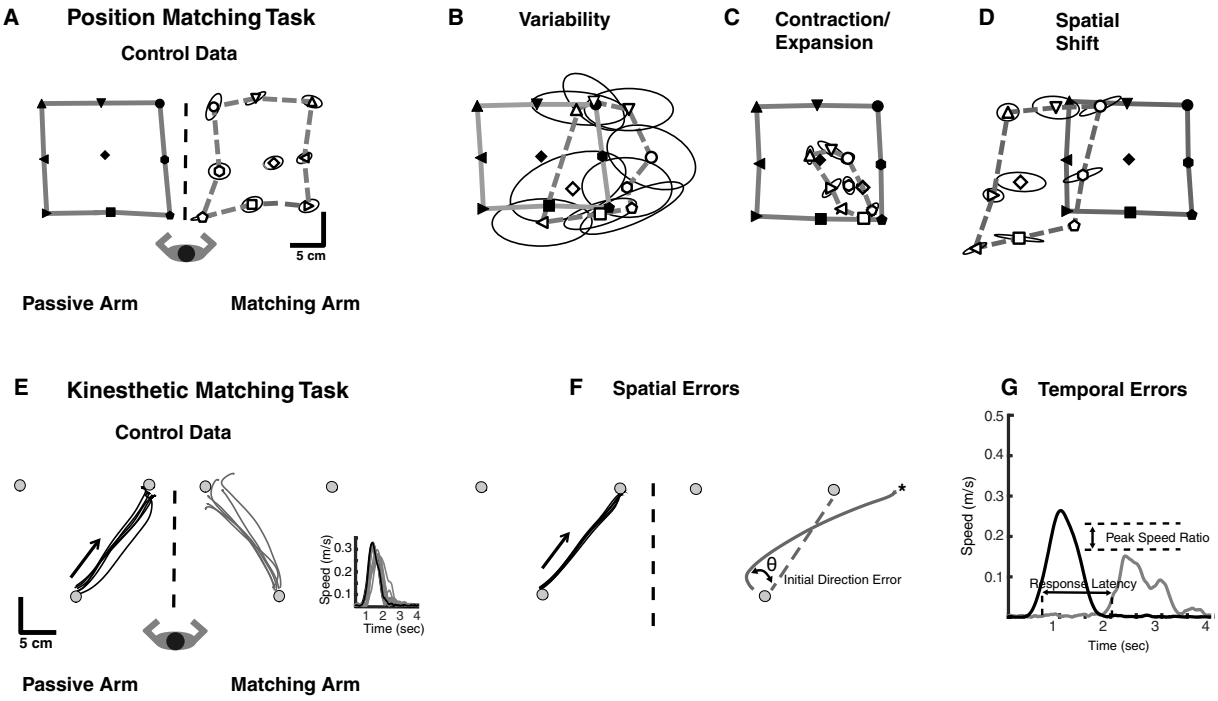

Fig. 1. Position and kinesthetic matching tasks.
A) Exemplar control data for the position matching task. In this example, the robot moved the control subject's passive left arm to one of 9 spatial locations (filled symbols) and the control subject mirror-matched the positions (open symbols) with their active right arm. A solid line joins the outer filled symbols to illustrate the workspace utilized by the arm passively moved by the robot. Similarly, a dashed line connects the unfilled symbols to represent the workspace where the subject actively matched. Trial-to-trial variability is symbolized by ellipses around each location – each ellipse represents one standard deviation. B) The performance of the subject's active arm has been mirrored onto the robotically moved passive arm. An exemplar stroke subject who demonstrated high variability is presented. C) An exemplar stroke subject who demonstrated a contracted sense of workspace. D) An exemplar stroke subject who demonstrated spatial shift of the workspace location to the left. E) Exemplar control data for the kinesthetic matching task. The robot moved the subject's passive left arm (black lines) and the subject actively mirror-matched the movement (grey lines) with the opposite arm as soon as they felt the robot move. The arrow refers to the direction that the passive arm was moved. Exemplar temporal data from a healthy control subject is also presented. F) Exemplar stroke subject data demonstrating initial direction error and abnormal path length ratio (*). G) Exemplar stroke subject data demonstrating slow response latency and slowed peak speed ratio.

locations, mirrored across the midline). Subjects moved a white circle that represented the tip of the index finger of their *active arm* into the red circle. This effectively brought the two limbs into a mirrored start position. The visual targets then extinguished and as soon as the subject felt the robot move the passive arm, they mirror-matched the direction, speed, and length of the robotic movement with their opposite (active) arm. Six movement directions (between the 3 locations) were completed 6 times for a total of 36 trials. If subjects did not complete the matching movement in 10 s, that trial was categorized as a non-movement. In participants with stroke the affected arm was only ever used as the *passive arm*. Controls completed the task twice with both arms each serving as the *passive arm* once.

Four patterns of errors (two temporal and two spatial) were quantified with the kinesthetic matching task for this study. All parameters have been previously described (Semrau et al., 2013a, 2013b). *Response latency* measured the difference in time between when the robot initiated the passive arm movement and the subject initiated the matching movement with the active arm. Movement initiation was defined as the point when subjects reached 10% of their maximum speed and had a positive-going acceleration. *Peak speed ratio* compared the subject's ability to match the speed of the robotically moved *passive arm*. A value of 1 indicated perfect speed matching and a value of < 1 indicated an active movement slower than the robotically-moved passive arm. *Initial direction error* parameter quantified the sense of direction. It is defined as the angular deviation between the movement paths of the subject's active arm and the passive arm from movement onset to peak hand speed. *Path length ratio* quantified the subject's ability to match the length of the movement. It was calculated by dividing the total movement length of the active arm by the length of the passive arm movement. A value of 1 indicated perfect matching whereas a value of < 1 indicated that the subject generated a movement shorter than that of the passively moved arm. An overall *task score* for the kinesthetic matching task was also calculated as detailed in Section 2.2.5.

2.2.4. Assessment of motor function

To ensure that altered motor control of the active, ipsilesional, arm did not hamper performance on the position and kinesthetic matching tasks, subjects also completed a visually guided reaching task. This task assessed the ability to make accurate and timely unassisted reaching movements (Coderre et al., 2010). With this centre-out task, the tip of the index finger was positioned within a centre target and held there for 1250–1750 ms until one of eight peripheral targets illuminated. Subjects had 3000 ms to reach to the target. Each of the eight targets were presented randomly within a block which was repeated eight times for 64 trials. In keeping with previous work from our group (Semrau et al., 2017), we considered subjects to have ipsilesional deficits if they scored outside of the normative range on the visually guided reaching task score (Section 2.2.5).

2.2.5. Normative scores for the robotic tasks

Stroke subject performance was compared to previously-collected control data on each task to permit comparisons within and between subjects. Control data for the position matching task was collected from 494 healthy subjects ranging in age from 18 to 93 years (mean = 50). Control data for the kinesthetic matching task was collected from 164 subjects who ranged in age from 18 to 93 (mean = 52). Control data for visually guided reaching was collected from 178 subjects between 19 and 83 years of age (mean 49). Control data was transformed to a *z*

score distribution for individual task parameters accounting for age, sex and handedness (BKIN Technologies, 2016; Kenzie et al., 2016; Semrau et al., 2013a, 2013b). If a stroke subject's score fell outside of the 95% normative range, their performance was considered abnormal and we refer to them as having abnormal proprioception. Scores > 1.65 were considered abnormal for one-tailed parameters (variability, spatial shift, response latency, initial direction error) and scores < −1.96 or > 1.96 were considered abnormal for two-tailed parameters (contraction/expansion, path length ratio, and peak speed ratio). Absolute values were used for the two-tailed parameters when conducting the lesion analyses (Section 2.5) in order to comply with the lesion analysis software.

An overall task score was also calculated based on the root-mean-square (RMS) of z scores for all task parameters (BKIN Technologies, 2016; Simmatis et al., 2017). As with task parameters, the RMS values were re-normalized based on performance of a large cohort of healthy controls. These scores were then transformed to positive values such that a task score of 0 represents best performance on a task while higher values indicate poorer performance. Task scores align with standard deviation (SD) percentiles of a normal distribution such that 1 SD = 68.3% and 2 SD = 95.4%. Task scores > 1.96 were considered abnormal.

Some subjects completed too few trials (≤ 17 movements with the active arm) in the kinesthetic matching task to generate an appropriate score (n = 23 subjects at the first timepoint, and n = 4 at the final timepoint). This occurred when subjects could not detect that their arm had been moved by the robot. In this case, the worst possible score observed in other subjects, for a given parameter, was assigned to the individual.

2.3. Clinical assessment

Stroke subjects completed a number of clinical assessments at the same time as the robotic assessment. The Thumb Localizing Test (TLT) was used to assess upper extremity position sense (Hirayama et al., 1999). For the TLT the subject closes their eyes while the examiner places and holds the subject's affected arm in the air. The subject is then asked to touch their thumb with their unaffected side. A score of 0–3 is determined (0 = accurately locates thumb, 3 = unable to locate thumb). The Modified Edinburgh Handedness Inventory is a self-report scale that was used to determine hand dominance (Oldfield, 1971). The Functional Independence Measure (FIM) provides a measure of an individual's level of independence for activities of daily living (Keith et al., 1987). Each activity (i.e. grooming, walking, problem solving) receives a maximum score of 7, indicating complete independence. The highest achievable score of 126 indicates that a subject is independent. The Modified Ashworth Scale (MAS) is a 5-point ordinal scale that measures spasticity (0 indicates normal muscle tone; 4 indicates contracture) (Bohannon and Smith, 1987). The Chedoke McMaster Stroke Assessment (CMSA) Impairment Inventory of the Arm and Hand is a 7-point ordinal scale that measures motor impairment. Subjects' attempt to perform several pre-determined movements and are scored between 0 and 7 (0 = flaccid arm to 7 = normal movement) (Gowland et al., 1993). The Behavioural Inattention Test was used to assess for visuospatial neglect (Wilson et al., 1988). Subjects performed the six conventional subtests and a score of 129 or less (out of 146) was considered to be consistent with visuospatial neglect.

2.4. Imaging

All subjects with stroke underwent MRI or CT according to standard clinical acute stroke protocol at the Foothills Medical Centre as soon as possible after stroke onset. MRI scans included T2-weighted fluid-attenuated inversion-recovery (FLAIR), diffusion-weighted sequences (DWI), and, when appropriate, gradient echo (GRE) or susceptibility weighted imaging (SWI). MR images were acquired using a 1.5 or 3 T General Electric (GE) Medical Systems scanner while CT scans were acquired on a Siemens System or one of three GE scanners. In cases where subjects had multiple imaging dates, we selected the closest date prior to the preliminary robotic assessment.

2.5. Lesion delineation and analysis

Trained assessors (SF and JK) manually delineated lesions on each axial slice of a subject's T2-weighted FLAIR or CT using MRIcron software (Rorden et al., 2007) (https://www.nitrc.org/plugins/mwiki/index.php/niistat:MainPage) to obtain a volume of interest (VOI) representative of the region of damaged tissue. When marking the lesions on MRI, DWI sequences were used to inform stroke damage due to ischemia and GRE or SWI images were used to identify hemorrhagic stroke. CT scans were used for subjects who did not have MRI as has been done in other lesion studies (Karnath et al., 2009; Verdon et al., 2010; Winder et al., 2015). Only CTs with well-defined lesions that were collected beyond the very acute stage post stroke were used (mean 2.8 days post-stroke). A stroke neurologist blinded to the robotic assessment scores (AY) verified the VOIs with the original imaging to ensure accuracy.

VOIs were normalized to the Montreal Neurological Institute (MNI) template using the clinical toolbox (http://www.nitrc.org/projects/clinicaltbx) (Rorden et al., 2012) with SPM8 (http//fil.ion.ucl.ac.uk/spm) (Friston et al., 1994). Cost function masks were used during normalization to prevent distortions due to signal alterations from the damaged tissue (Brett et al., 2001). The normalized VOIs were compared to the original imaging to ensure accuracy and were used in subsequent lesion analyses. Consistent with similar studies interrogating nonlateralized function, left-hemisphere VOIs were mirrored across the midsagittal axis (Globas et al., 2011; Kuper et al., 2011; Lo et al., 2010; Meyer et al., 2016a; Zhu et al., 2010).

2.5.1. Lesion analyses

To determine the impact of cortical/sub-cortical lesion location on the performance of the robotic proprioceptive tasks, the normalized lesions were analyzed with both statistical Region of Interest (sROI) analysis and lesion frequency mapping. These analyses are complementary as sROI identifies lesion/behaviour relationships at the regional level (Findlater et al., 2016) while lesion frequency mapping identifies locations where voxels are more frequently damaged in subjects with the deficit of interest (de Haan and Karnath, 2017). Both analyses were conducted in subjects with cortical and/or subcortical lesions to identify brain regions associated with poor performance on the position matching and kinesthetic parameters.

Subjects with brainstem or cerebellar lesions were not included in the sROI or lesion frequency analyses because the group numbers were too small. However, given that little is known about proprioceptive recovery in these subjects, we included them in the behavioural analysis (Fig. 2).

2.5.1.1. Statistical region of interest. We used NiiStat (http://www.nitrc.org/projects/niistat) to conduct the sROI analysis. One hundred and fifty regions were defined using the Automated Anatomical Labeling Atlas (AAL) (Tzourio-Mazoyer et al., 2002) for cortical and subcortical regions in addition to white matter regions defined by the Neuroanatomy and Tractography Laboratory atlases (http://www.natbrainlab.com) (Catani and Thiebaut de Schotten, 2008). For sROI analyses, each voxel mapped to a single region or tract. If a voxel mapped to a region where the AAL and tractography atlases overlapped, the voxel was assigned to the tractography atlas (Findlater et al., 2016). In cases where a voxel had equal probability to be from either of two overlapping tracts, the voxel was randomly assigned one of the two labels.

Only regions where a minimum of 10% of subjects had lesions were analyzed (Sperber and Karnath, 2018). The proportion of ROI damage

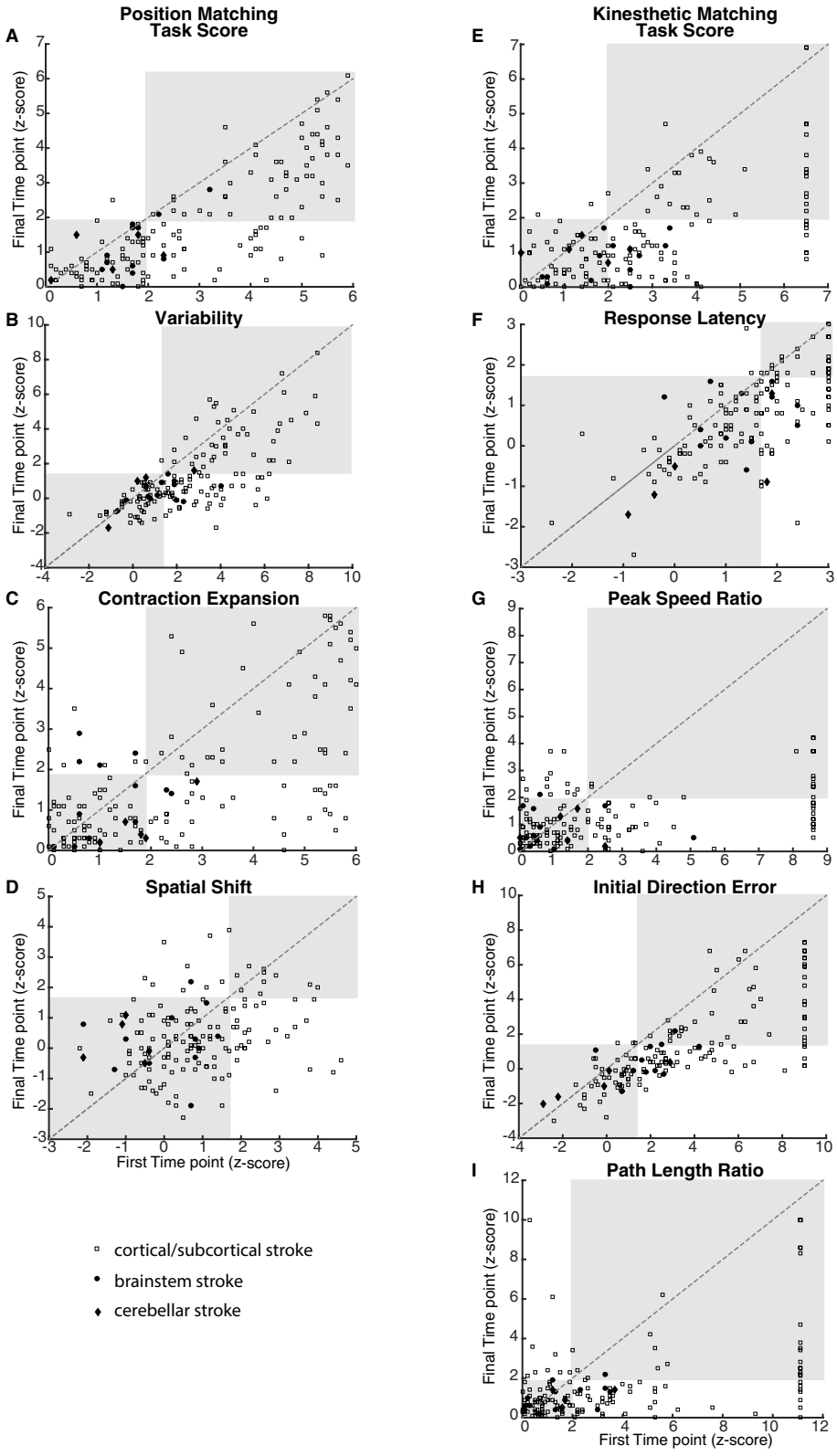

Fig. 2. Recovery plots.
Recovery plots of the position (A-D) and kinesthetic (*E*-I) matching tasks. First timepoint z-scores are plotted on the x axis, final timepoint scores are plotted on the y axis. The unfilled squares represent subjects with cortical and/or subcortical stroke, filled circles represent subjects with brainstem stroke, and filled diamonds represent subjects with cerebellar stroke. Grey boxes demonstrate the recovery categories – the bottom left quadrant contains subjects who score within the normative range at both timepoints, the bottom right quadrant contains subjects who are abnormal at the first timepoint and recover at the final timepoint, the top right quadrant contains subjects who are abnormal at both timepoints, and the upper left quadrant contains subjects who are normal at the first timepoint but are abnormal at the final timepoint.

was calculated for each subject and entered into a general linear model. The model then tested whether the proportion of damage to a region was significantly associated with poor position matching or kinesthetic matching scores. The results were converted to a z-score for each region. The data were permuted 4000 times to control for family-wise error and establish a significance threshold of $p < .05$ (Rorden et al., 2007).

2.5.1.2. Lesion frequency analysis. In addition to sROI, a voxelwise lesion frequency analysis was conducted using MRIcron (https//: www.nitrc.org/projects/mricron) in order to increase spatial specificity. For the lesion frequency analysis, subjects were divided into sub-categories based on their position and kinesthetic matching task scores (no-deficit, recover, and persistent deficits). The percentage of subjects who had 'no-deficit' (who were within the normative range

Table 1
Sample characteristics.

Subjects with cortical and/or subcortical lesions (n = 136)	56L; 80R	
Age (mean; range)	59.4; 25-86	
Sex	43F; 93M	
Stroke Territory		
[ACA,MCA,PCA,ACA + MCA,MCA + PCA]	[5,106,18,4,3]	
Lesion Volume (mL)	37.2 (53.4)	
Handedness	8L; 128R	
TLT [0,1,2,3]	[55,40,27,12]**	[88,36,8,4]
FIM	94.5(24.5)	120.9(7.7)
MAS [0,1,1$^+$,2,3,4] affected UE	[102,18,9,6,0,0]*	[97,16,2,12,9,0]
CMSA [7,6,5,4,3,2,1] affected UE	[43,17,24,8,19,12,13]	[80,17,16,5,14,2,2]
Less-affected UE	[112,23,1,0,0,0,0]	[129,5,1,1,0,0,0]
Neglect (number of subjects)	28	6
Subjects with brainstem lesions (n = 12)	3L; 9R	
Age (mean; range)	57.8 (25–80)	
Sex	5F; 7M	
Stroke Territory		
[PCA, BA,VA]	[3,6,3]	
Lesion Volume (mL)	0.60 (0.5)	
Handedness	1L; 11R	
TLT [0,1,2,3]	[5,4,2,1]	[10,2,0,0]
FIM	91.8 (19.2)	119.2 (9.8)
MAS [0,1,1$^+$,2,3,4] affected UE	[10,2,0,0,0,0]	[8,2,0,1,1,0]
CMSA [7,6,5,4,3,2,1] affected UE	[1,2,2,1,3,3,0]	[6,2,1,2,1,0,0]
Less-affected UE	[10,1,1,0,0,0,0]	[12,0,0,0,0,0,0]
Neglect (number of subjects)	1	0
Subjects with cerebellar lesions (n = 5)	1L; 4R	
Age (range)	53.4 (31–67)	
Sex	5M	
Stroke Territory		
[SCA, PICA]	[2,3]	
Lesion Volume (mL)	14.4 (14)	
Handedness	1L; 4R	
TLT [0,1,2,3]	[2,3,0,0]	[4,1,0,0]
FIM	112.4 (17.6)	125.8 (0.4)
MAS [0,1,1$^+$,2,3,4] affected UE	[5,0,0,0,0,0]	[5,0,0,0,0,0]
CMSA [7,6,5,4,3,2,1] affected UE	[2,3,0,0,0,0,0]	[5,0,0,0,0,0,0]
Less-affected UE	[5,0,0,0,0,0,0]	[5,0,0,0,0,0,0]
Neglect (number of subjects)	0	0

Abbreviations: F/M, female, male; R/L, right, left; ACA/MCA/PCA, anterior, middle, posterior cerebral artery respectively; BA, basilar artery; VA, vertebral artery; SCA, superior cerebellar artery; PICA, posterior inferior cerebellar artery.
Unless otherwise noted, mean is followed by standard deviation in brackets. When appropriate, two columns of data are presented– the first time point is on the left, the final time point is on the right. Abbreviations defined in text: TLT, Thumb Localizing Test; FIM, Functional Independence Measure; MAS, Modified Ashworth Scale; CMSA, Chedoke-McMaster Stroke Assessment.

* Data unavailable for one subject.

** Data unavailable for two subjects.

Table 2
Subjects impaired on each parameter and recovery categories.

Parameter	First Time point	Recovery categories			
		No Deficit	Recovered	Persistent Deficit	Worse
Position Match					
TS	86 (82)	66 (53)	32 (30)	54 (52)	1 (1)
VAR	92 (86)	60 (49)	51 (45)	42 (42)	0 (0)
CE	76 (73)	68 (58)	35 (32)	42 (42)	8 (4)
SS	39 (39)	104 (88)	29 (29)	11 (11)	9 (8)
Kinesthesia					
TS	93 (85)	58 (49)	56 (50)	34 (34)	3 (3)
RL	72 (66)	77 (66)	45 (39)	29 (29)	2 (2)
PSR	61 (58)	79 (66)	46 (43)	13 (13)	14 (14)
IDE	98 (90)	55 (46)	54 (47)	42 (42)	1 (1)
PLR	77 (71)	67 (56)	50 (46)	25 (23)	11 (11)

Numbers outside of the brackets indicate the number of subjects out of 153 who scored outside the normative range. Numbers within brackets indicate the subjects with cortical and/or subcortical lesions that were included in the sROI and subtraction analyses. Abbreviations: TS, task score; VAR, variability, CE, contraction/expansion; SS, spatial shift; RL, response latency; PSR, peak speed ratio; IDE, initial direction error; PLR, path length ratio.

at both time points) was subtracted from the percentage of subjects with 'persistent' deficits (outside the normative range at both time points). The results are displayed on a frequency map that identifies voxels damaged more frequently in subjects with persistent deficits (de Haan and Karnath, 2017). Only voxels damaged at least 20% more often in subjects with persistent deficits were considered (Lunven et al., 2015). Subjects who demonstrated poor performance initially, but then 'recovered' to within the normative range, or the rare subjects whose initial performance was within the normative range but was outside that range at the final time point were not included in this analysis. Since performance varied across parameters, overlay maps were created for the no-deficit and persistent deficit groups for each parameter. This type of analysis has been used previously to examine visuospatial neglect (Karnath et al., 2002) (Karnath et al., 2002), depression (Kim et al., 2017), and motor skill recovery (Abela et al., 2012) after stroke.

2.6. Statistical analyses

Descriptive statistics were used to describe subject characteristics. One-way ANOVA and post hoc t-tests were employed to determine if the three patient subgroups (no-deficit, recovered, persistent) differed in

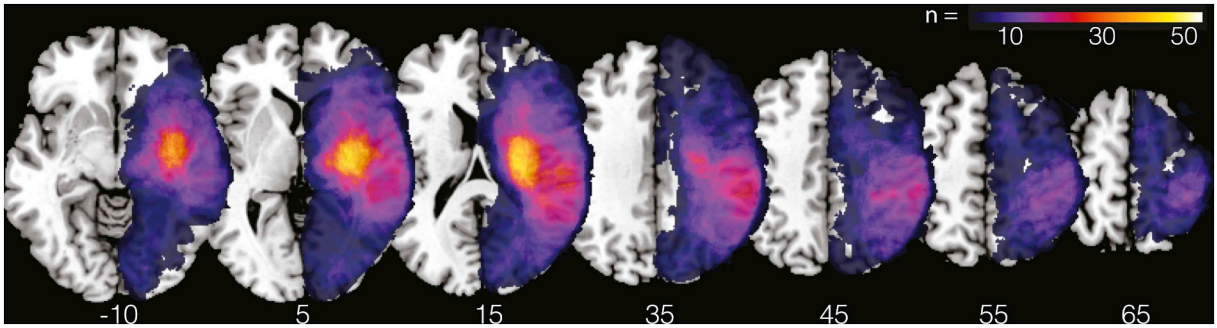

Fig. 3. Lesion overlap map.
Lesion overlap map for 136 subjects included in the sROI analysis. The scale bar indicates the number of subjects' lesions overlapping in a given area. MNI z-coordinates are presented below their respective transverse sections.

age, timing from stroke to first assessment, or lesion volume. Pearson correlations were conducted to measure the relationship between robotic parameters. Bonferroni corrections were employed to control for multiple comparisons.

3. Results

3.1. Subject characteristics

The demographic characteristics and clinical scores for all subjects with stroke (n = 153) at study entry are presented in Table 1. The mean time between stroke onset and neuroimaging was 2.7 (SD ± 4.0) days. One hundred and ten subjects received MRIs while 43 received CT scans. One hundred thirty-two subjects had ischemic stroke and 21 had hemorrhagic stroke. The mean time between stroke and robotic/clinical data collection for the first time point was 11.4 ± 8 days post-stroke and 171.1 ± 39 days for the final time point.

3.2. Robotic measurement of position sense and kinesthesia

Fig. 2 presents the recovery plots of all subjects in both the position and kinesthetic matching tasks. Group performance for all 153 subjects on the individual position and kinesthetic matching task parameters for the first and final time points is presented in Table 2. To summarize, 56% of subjects demonstrated abnormal position sense initially and in 40% this persisted at the final time point (based on task score). Similarly, the majority of subjects initially demonstrated abnormal kinesthesia based on task score (61%), however, this only persisted in 25% of the subjects at the final time point.

A small portion of our sample had brainstem (n = 12) or cerebellar (n = 5) lesions. Detailed results for these subjects are also presented in Fig. 2. In the subjects with brainstem lesions, 25% had abnormal position sense initially and 17% persisted at the final timepoint (based on task score). In this same group 67% had abnormal kinesthesia initially and this decreased to 17% by the final time point. In the subjects with cerebellar lesions, 1 subject had abnormal position sense initially and none had deficits at the final timepoint. In this same group 2 subjects had abnormal kinesthesia initially and this decreased to none by the final time point. Details of performance on the individual parameters for both of these groups can be seen in Fig. 2.

3.3. Lesion analyses

Of the 136 subjects who had cortical and subcortical lesions, 39% had no-deficits at either time point, 22% recovered, and 38% had persistent deficits (according to the position matching task score). We investigated whether these subcategories of subjects were different in age, time from stroke onset to initial robotic assessment, or lesion volume using one-way analysis of variance (ANOVA) and post-hoc testing. Age was not different between any of the groups. The no-deficit and recover groups were not different across the three factors. However, the group with persistent deficits was significantly different from both the no-deficit and recover groups in terms of time from stroke onset to assessment [$F(2) = 6.98$, $p = .001$] and lesion volume [$F(2) = 16.1$, $p \leq .001$]. On average, subjects with persistent deficits completed the robotic assessment later (mean 14.5 days ± 10.7) compared to the no-deficit or recover groups (9.2 ± 6.9 and 8.6 ± 6.0 respectively). Subjects with persistent deficits also had greater lesion volume (mean 65.4 mL ± 65.9) compared to the no-deficit and recover groups (15.2 mL ± 29.1 and 23.2 mL ± 34.3 respectively). We then repeated the above analysis for the kinesthetic matching task score and found similar results in both the ANOVA and post-hoc testing.

3.3.1. sROI analysis

Lesion overlap maps (Fig. 3) of subjects with cortical/sub-cortical lesions (n = 136) demonstrated that the greatest lesion distribution was in the posterior putamen (n = 49).

Table 3 details the sROI analysis results identifying statistically significant ($p < .05$) relationships between lesion locations and abnormal position (Fig. 4) and kinesthetic matching (Fig. 5) scores at the first and final time points. Across both tasks, more regions tended to be associated with damage at the first time point than the final time point. Spatial shift was the only parameter that had more regions associated with poor performance at the final timepoint than the first timepoint.

For the remainder of this section, final time point results will be discussed as we are interested in which damaged regions of the brain lead to persistent stroke-related impairments in proprioception.

At the final timepoint we observed statistically significant ($p < .05$) relationships between both the position and kinesthetic matching tasks scores and the supramarginal gyrus, Heschl's gyrus, and the arcuate fasciculus. These brain regions were also found to have significant relationships with all parameters other than peak speed ratio, although these regions were present in uncorrected maps ($p > .05$) for this parameter.

Of note, in order to ensure that our results were not impacted by subjects with ipsilesional motor deficits, sROI analyses were repeated excluding those subjects (n = 14) with ipsilesional deficits on the visually guided reaching task. Doing so did not significantly change the results seen in Figs. 4, 5, or Table 3 (Supplementary Fig. 1).

3.3.2. Lesion frequency analysis

Abnormal performance on the individual parameters for the position and kinesthetic matching tasks was associated with damage to similar brain regions. For improved spatial specificity, we employed a lesion frequency analysis for each individual parameter at the final time point for position matching (Fig. 6) and kinesthetic matching (Fig. 7). When frequency maps were superimposed, the supramarginal gyrus, arcuate fasciculus, and Heschl's gyrus were all associated with

Table 3
AAL and Catani atlas-based regions and z-scores associated with poor scores on individual parameters and task scores of the position and kinesthetic matching tasks.

First Time Point		Final Time Point	
Region	z-score	Region	z-score
Position Matching – Task Score			
Arcuate fasciculus	6.0	Arcuate fasciculus	6.1
Heschl's gyrus	5.7	Heschl's gyrus	5.7
Cortico_Spinal Tract	5.2	Supramarginal gyrus	5.7
SupraMarginal gyrus	5.2	Postcentral gyrus	5.3
Postcentral gyrus	5.2	Parietal_Inferior gyrus	5.2
Optic_Radiations	5.2	Angular gyrus	4.6
Internal_Capsule	4.8	Temporal_Superior gyrus	4.5
Parietal_Inferior gyrus	4.8	Posterior_Segment	4.2
Temporal_Superior gyrus	4.8	Rolandic_Operculum	4.2
Anterior_Segment	4.2	Optic_Radiations	4.2
Rolandic_Operculum	4.1	Anterior_Segment	3.8
Angular gyrus	4.1	Parietal_Superior gyrus	3.8
Posterior_Segment	4.1	Temporal_Middle gyrus	3.6
Cortico_Ponto_Cerebellum	4.0	Cortico_Spinal Tract	3.6
Long_Segment	3.9	Internal_Capsule	3.5
Insula	3.8	Putamen	3.2
Temporal_Middle gyrus	3.8	Long_Segment	3.1
Parietal_Superior gyrus	3.8	Insula	3.0
Putamen	3.5		
Precentral gyrus	3.4		
Inferior_Longitudinal_Fasciculus	3.0		
Variability			
Arcuate fasciculus	5.2	Arcuate fasciculus	5.6
Heschl's gyrus	4.8	Heschl's gyrus	5.6
SupraMarginal gyrus	4.5	Supramarginal gyrus	5.3
Cortico_Spinal Tract	4.5	Temporal_Superior gyrus	4.6
Postcentral gyrus	4.2	Angular gyrus	4.4
Rolandic_Operculum	4.2	Rolandic_Operculum	4.3
Anterior_Segment	4.2	Parietal_Inferior gyrus	4.3
Parietal_Inferior	4.1	Posterior_Segment	4.3
Precentral gyrus	4.0	Temporal_Middle gyrus	4.3
Optic_Radiations	4.0	Postcentral gyrus	3.9
Internal_Capsule	3.9	Optic_Radiations	3.9
Temporal_Superior gyr	3.9	Anterior_Segment	3.8
Insula	3.7	Insula	3.5
Posterior_Segment	3.6	Putamen	3.2
Angular gyrus	3.6	Occipital_Middle gyrus	3.0
Frontal_Inferior Operculum	3.4		
Long_Segment	3.3		
Frontal_Middle gyrus	3.2		
Frontal_Inferior gyrus (triangular)	3.1		
Putamen	3.0		
Temporal_Middle gyrus	3.0		
Contraction/Expansion			
Heschl's gyrus	4.8	Postcentral gyrus	4.3
Postcentral gyrus	4.7	Parietal_Superior gyrus	3.9
Arcuate fasciculus	4.5	Parietal_Inferior gyrus	3.9
Cortico_Spinal Tract	4.4	Arcuate fasciculus	3.8
Optic_Radiations	4.3	Heschl's gyrus	3.4
Temporal_Superior gyrus	4.1	SupraMarginal gyrus	3.3
SupraMarginal gyrus	4.1	Superior_Cerebellar_Peduncle	3.2
Internal_Capsule	3.9	Angular gyrus	3.1
Cortico_Ponto_Cerebellum	3.7	Internal_Capsule	3.1
Parietal_Inferior gyrus	3.7	Cortico_Spinal Tract	3.0
Parietal_Superior gyrus	3.6		
Anterior_Segment	3.3		
Temporal_Middle gyrus	3.2		
Angular gyrus	3.2		
Rolandic_Operculum	3.1		
Long_Segment	3.1		
Putamen	3.1		
Insula	3.0		
Spatial Shift			
Arcuate fasciculus	3.6	Arcuate fasciculus	4.7
Optic_Radiations	3.5	Supramarginal gyrus	4.6
Heschl's gyrus	3.2	Parietal_Inferior gyrus	4.3
Postcentral gyrus	2.9	Parietal_Superior gyrus	4.0

(*continued on next page*)

Table 3 (*continued*)

First Time Point		Final Time Point	
Region	z-score	Region	z-score
SupraMarginal gyrus	2.9	Heschl's gyrus	4.0
		Optic_Radiations	3.7
		Posterior_Segment	3.6
		Postcentral gyrus	3.5
		Temporal_Superior gyrus	3.5
		Angular gyrus	3.5
		Rolandic_Operculum	3.2
Kinesthetic Matching – Task Score			
Arcuate fasciculus	5.6	Heschl's gyrus	4.8
Heschl's gyrus	5.4	Arcuate fasciculus	4.5
Cortico_Spinal Tract	5.2	Supramarginal gyrus	4.2
SupraMarginal gyrus	4.8	Parietal_Inferior gyrus	3.9
Postcentral gyrus	4.7	Postcentral gyrus	3.7
Optic_Radiations	4.6	Angular gyrus	3.3
Internal_Capsule	4.5	Parietal_Superior gyrus	3.2
Parietal_Inferior gyrus	4.4	Temporal_Superior gyrus	3.2
Temporal_Superior gyrus	4.1		
Cortico_Ponto_Cerebellum	4.0		
Long_Segment	4.0		
Anterior_Segment	3.9		
Insula	3.8		
Angular gyrus	3.8		
Rolandic_Operculum	3.7		
Posterior_Segment	3.5		
Parietal_Superior gyrus	3.3		
Putamen	3.2		
Temporal_Middle gyrus	2.9		
Response Latency			
Heschl's gyrus	6.7	Arcuate fasciculus	5.0
Arcuate fasciculus	6.3	Heschl's gyrus	4.8
Optic_Radiations	6.1	Supramarginal gyrus	4.6
Cortico_Spinal Tract	5.8	Posterior_Segment	4.2
SupraMarginal gyrus	5.4	Temporal_Superior gyrus	4.2
Temporal_Superior gyrus	5.3	Optic_Radiations	4.1
Internal_Capsule	5.3	Parietal_Inferior gyrus	3.9
Insula	5.3	Angular gyrus	3.7
Cortico_Ponto_Cerebellum	4.9	Parietal_Superior gyrus	3.5
Anterior_Segment	4.9	Postcentral gyrus	3.4
Postcentral gyrus	4.9	Temporal_Middle gyrus	3.3
Long_Segment	4.8	Internal_Capsule	3.2
Rolandic_Operculum	4.8	Cortico_Spinal Tract	3.2
Parietal_Inferior gyrus	4.6	Rolandic_Operculum	2.9
Posterior_Segment	4.3		
Angular gyrus	4.0		
Temporal_Middle gyrus	4.0		
Putamen	4.0		
Parietal_Superior gyrus	3.3		
Temporal_Pole_Sup_R	3.2		
Inferior_Occipito_Frontal_Fasciculus	3.2		
Inferior_Longitudinal_Fasciculus	3.2		
Uncinate	3.1		
Thalamus_R	3.0		
Fornix	3.0		
Pallidum	2.9		
Frontal_Inferior gyrus (triangular)	2.9		
Precentral gyrus	2.9		
Peak Speed Ratio			
Arcuate fasciculus	5.0	Postcentral gyrus	3.9
Parietal_Inferior gyrus	4.8	Parietal_Superior gyrus	3.9
SupraMarginal gyrus	4.6	Cortico_Spinal Tract	3.3
Postcentral gyrus	4.5		
Heschl's gyrus	4.0		
Angular gyrus	4.0		
Parietal_Superior gyrus	3.7		
Optic_Radiations	3.1		
Initial Direction Error			
Arcuate fasciculus	5.7	Arcuate fasciculus	4.7
Heschl's gyrus	5.2	Heschl's gyrus	4.5
Postcentral gyrus	5.1	Postcentral gyrus	4.3
SupraMarginal gyrus	4.9	Supramarginal gyrus	4.2
Optic_Radiations	4.5	Cortico_Spinal Tract	4.0

(*continued on next page*)

Table 3 (*continued*)

First Time Point		Final Time Point	
Region	z-score	Region	z-score
Cortico_Spinal Tract	4.5	Parietal_Superior gyrus	4.0
Parietal_Inferior gyrus	4.4	Parietal_Inferior gyrus	3.9
Angular gyrus	4.0	Optic_Radiations	3.9
Parietal_Superior gyrus	3.9	Internal_Capsule	3.7
Internal_Capsule	3.9	Angular gyrus	3.6
Temporal_Superior gyrus	3.9	Cortico_Ponto_Cerebellar tract	3.3
Cortico_Ponto_Cerebellum	3.7	Posterior_Segment	3.2
Long_Segment	3.6	Temporal_Superior gyrus	3.0
Anterior_Segment	3.6		
Posterior_Segment	3.5		
Rolandic_Operculum	3.4		
Insula	3.2		
Path Length Ratio			
Arcuate fasciculus	5.7	Arcuate fasciculus	3.5
Heschl's gyrus	4.9	Heschl's gyrus	3.6
SupraMarginal gyrus	4.8	Supramarginal gyrus	3.7
Cortico_Spinal Tract	4.6		
Parietal_Inferior gyrus	4.5		
Postcentral gyrus	4.4		
Optic_Radiations	4.2		
Internal_Capsule	3.9		
Angular gyrus	3.8		
Cortico_Ponto_Cerebellum	3.8		
Temporal_Superior gyrus	3.6		
Long_Segment	3.5		
Posterior_Segment	3.2		
Anterior_Segment	3.1		
Insula	3.0		

abnormal performance across the position and kinesthetic matching parameters.

4. Discussion

The goal of this study was to improve our understanding of proprioceptive recovery post stroke. Here, we aimed to identify the lesion locations associated with persistent proprioceptive impairment and to determine whether subcomponents of proprioception had unique lesion locations. We found that proprioceptive deficits persisted into the chronic stage post stroke in a sizeable proportion of individuals (40% for position and 27% for kinesthetic matching). While lesion locations associated with persistent proprioceptive deficits varied slightly across task and parameter scores, a common trend emerged in both the sROI and lesion frequency analyses. The supramarginal gyrus, arcuate fasciculus, and Heschl's gyrus were associated with poor performance in both position and kinesthetic matching, indicating that these areas are likely part of a distributed network involved in processing proprioception that extends beyond primary somatosensory cortex. Given the likelihood that they are part of the same network, it follows that lesion locations were common across the two subcomponents of proprioception.

Several previous studies have assessed incidence of upper extremity proprioceptive deficits within a few weeks after stroke onset. Winward et al. (2002) assessed the elbow, wrist, thumb or finger of 100 subjects approximately 6 weeks post stroke and reported an incidence of 52%. Similarly, Carey and Matyas (2011) reported an incidence of 49% at an average of 50 days post stroke in 51 subjects. In these studies, the incidence of proprioceptive deficits in the early phase post-stroke is slightly less than our 2-week findings of 56% for position sense and 59% for kinesthesia. These differences, in part, are likely attributed to our sample being assessed several weeks earlier.

In the few longitudinal studies available, estimates of proprioceptive recovery have been more variable. In our study 20% of subjects had recovery in position sense and 37% of subjects had recovery in kinesthesia. A small longitudinal study ($n = 9$) reported higher (66%) proprioceptive recovery, but proprioception of the upper and lower body was combined and 8 subjects scored 60% intact or greater at the initial assessment (Winward et al. (2007). Connell et al. (2008) examined relative recovery in four somatosensory domains and reported that upper limb proprioception significantly improved by 6 months. However, the proportion of subjects that recovered was not specified. Meyer et al. (2016a, 2016b) found that persistent proprioceptive deficits ranged from 5% (Erasmus-modified Nottingham Sensory Assessment) to 50% (Thumb Finding Test, TFT). Their results on the TFT are similar to our finding of the TLT, where we observed that 50% of our subjects had impairments on the TLT. Our findings further expand on the knowledge of proprioceptive recovery by reporting that a large number of individuals have proprioceptive impairment on both robotic and clinical measures at 6 months post-stroke.

An important consideration when making comparisons to previous studies is that the robotic tasks we used to assess proprioception require several processes to complete the tasks. For example, performance on the kinesthetic task requires the subject to feel the initiation of movement, react to it, initiate a matching movement with the opposite arm, then match the speed, direction, and amplitude of the passive arm. This task, and the position sense task, require interhemispheric connections in order to achieve success. The tasks were based on assessments performed in healthy individuals (Goble and Brown, 2009; Goble et al., 2006) and traditional clinical assessments, such as the Modified Nottingham Sensory Assessment that assesses appreciation of movement, direction of movement, and joint position sense simultaneously (Lincoln et al., 1998). Importantly, this type of assessment is considered best-practice for patients with stroke (Academy of Neurologic Physical Therapy, 2011).

In the present study, subjects who had persistent proprioceptive deficits also had greater lesion volume. While lesion volume has been associated with poor recovery (Löuvbld et al., 1997; Saunders et al., 1995), a more recent view is that lesion volume is not predictive of recovery without the addition of lesion location (Chen et al., 2000; Feng

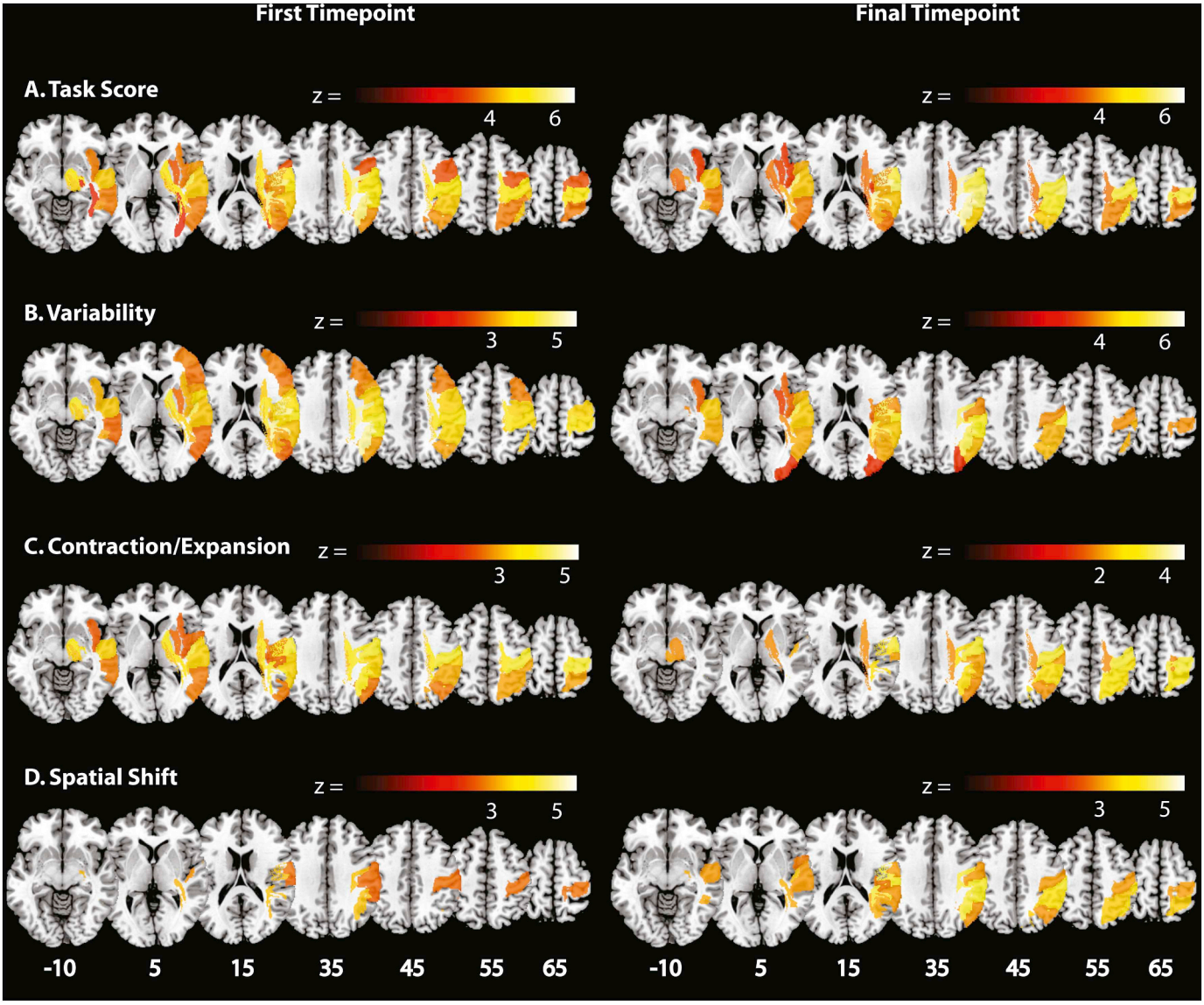

Fig. 4. Position matching task sROI results.
First and final time point statistical ROI results for the position match parameters for 136 subjects (excluding those with brainstem or cerebellar lesions) are presented. All regions presented surpassed correction permutation thresholding of $p < .05$. Scale bars are presented indicating the z-score, brighter regions are more associated with worse performance. A) Task Score B) Variability C) Contraction/Expansion D) Spatial Shift. MNI z-coordinates are presented below their respective transverse sections.

et al., 2015; Zhu et al., 2010), nor does it relate specifically to sensory, motor, or cognition (Hawe et al., 2018).

At 6 months post-stroke our sROI analysis found that lesion locations associated with persistent proprioceptive deficits were mainly constrained to similar regions across all proprioceptive parameters whereas previous studies have shown lesion locations associated with early proprioceptive deficits were more variable. Our group previously found that acute position matching deficits were associated with damage in the postcentral gyrus, the superior and inferior parietal gyri, the transverse temporal (Heschl's) gyrus, the posterior insula and the arcuate fasciculus (Findlater et al., 2016). Acute kinesthetic matching deficits were related to damage in the postcentral gyrus, supramarginal gyrus, insula, superior temporal gyrus, and parietal operculum (Kenzie et al., 2016). Another group using voxel-based lesion symptom mapping in an acute stroke model found that damage to the parietal operculum, posterior insula, and corona radiata were associated with poor proprioception (Meyer et al., 2016b). Overall, these 3 studies have similar findings in the acute phase post-stroke. Results from our current study suggest that the diversity of lesion locations associated with proprioceptive deficits in the first few weeks post-stroke tends to be reduced to fewer key regions (the supramarginal gyrus, arcuate fasciculus, and Heschl's gyrus) associated with persistent proprioceptive deficits. Differences in lesion/behaviour associations from early to chronic time points have also been reported in longitudinal studies of visuospatial neglect and motor recovery post-stroke (Abela et al., 2012; Karnath et al., 2011; Lunven et al., 2015; Wu et al., 2015). A recent study by Karnath and Rennig (2017) suggested that studies aiming to uncover the neural correlates of a behaviour should pair acute imaging and behavioural assessment whereas studies aiming to predict chronic deficits should pair acute imaging and chronic behavioural assessment. This is a subtle, but important difference and the aim of our study was in line with the latter.

Our results indicate that lesions in the supramarginal gyrus, the arcuate fasciculus, and Heschl's gyrus are associated with persistent deficits across all position and kinesthetic matching parameters. The supramarginal gyrus is part of the parietal association area where

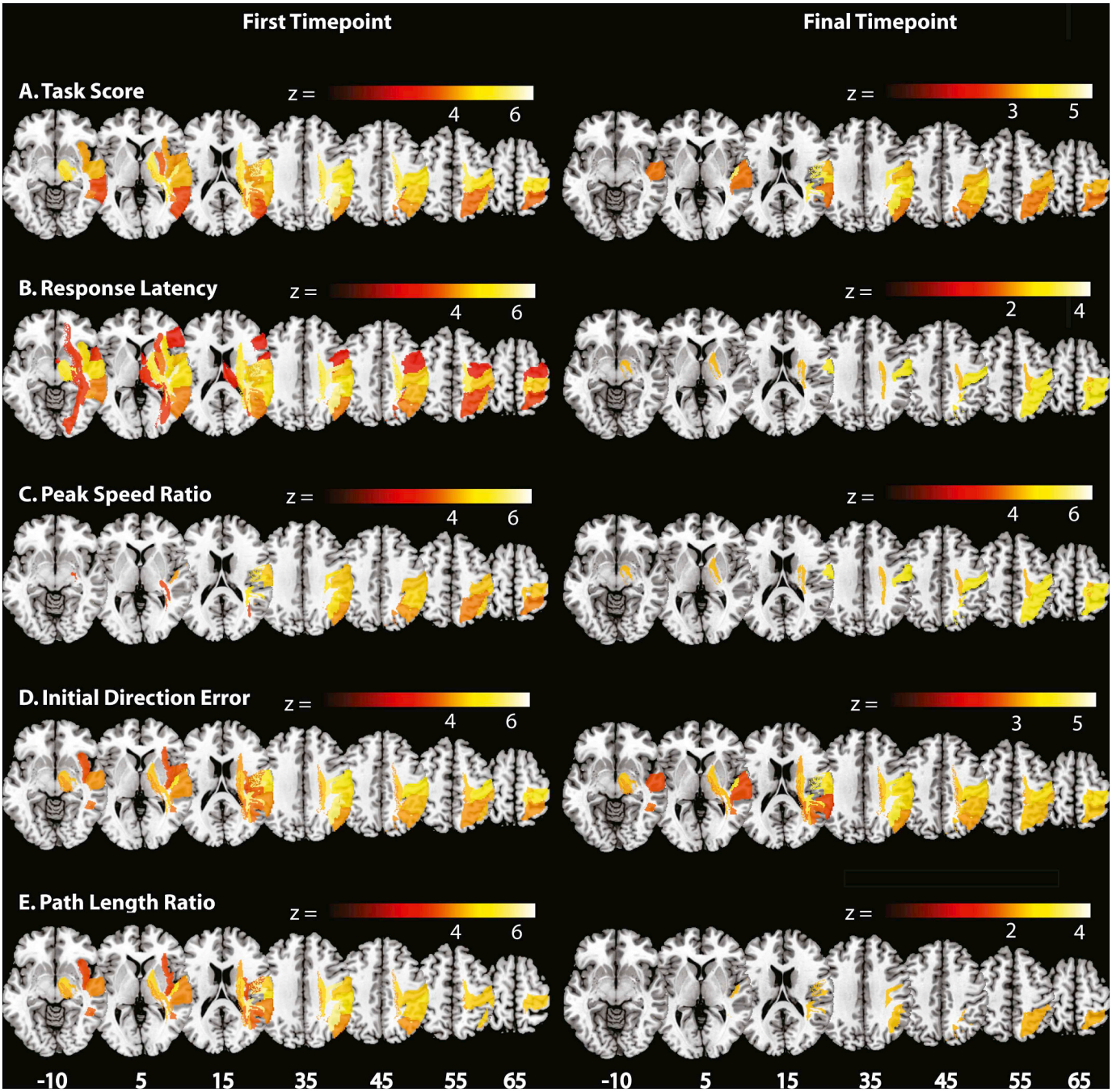

Fig. 5. Kinesthetic matching task sROI results.
First and final time point sROI results for the kinesthetic matching parameters for 136 subjects (excluding those with brainstem or cerebellar lesions) are presented. All regions presented surpassed correction permutation thresholding of $p < .05$. Scale bars are presented indicating the z-score, brighter regions are more associated with abnormal performance. A) Task Score B) Response Latency C) Peak Speed Ratio D) Initial Direction Error E) Path Length Ratio. MNI z-coordinates are presented below their respective transverse sections.

somatosensory information is integrated (Iwamura, 2003; Pandya and Seltzer, 1982). Functional MRI studies have found that the supramarginal gyrus plays an important role in awareness of hand position in healthy subjects (Ben-Shabat et al., 2015; Brozzoli et al., 2011) and stroke subjects (Ben-Shabat et al., 2015).

Recent diffusion MRI tractography studies have refined and expanded our understanding of the arcuate fasciculus beyond the classic notion of a pathway connecting Broca's and Wernicke's areas. The arcuate fasciculus is often considered a partition of the superior longitudinal fasciculus (Dick and Tremblay, 2012) and recent tractography studies have delineated it into three distinct segments (Catani et al., 2005; Thiebaut De Schotten et al., 2011). While the role of the arcuate fasciculus for language has been well documented, it also appears that the arcuate fasciculus/superior longitudinal fasciculus is important for processing upper limb position information for perception and goal-directed movement (Goldenberg and Karnath, 2006; Leiguarda and Marsden, 2000). It is therefore fitting that our findings indicate that the arcuate fasciculus is important for proprioceptive perception.

Heschl's gyrus was also associated with poor proprioceptive matching in our study. This area is also called the transverse temporal gyrus and corresponds with the primary auditory cortex (Wasserthal et al., 2014). In addition to various aspects of hearing, sound

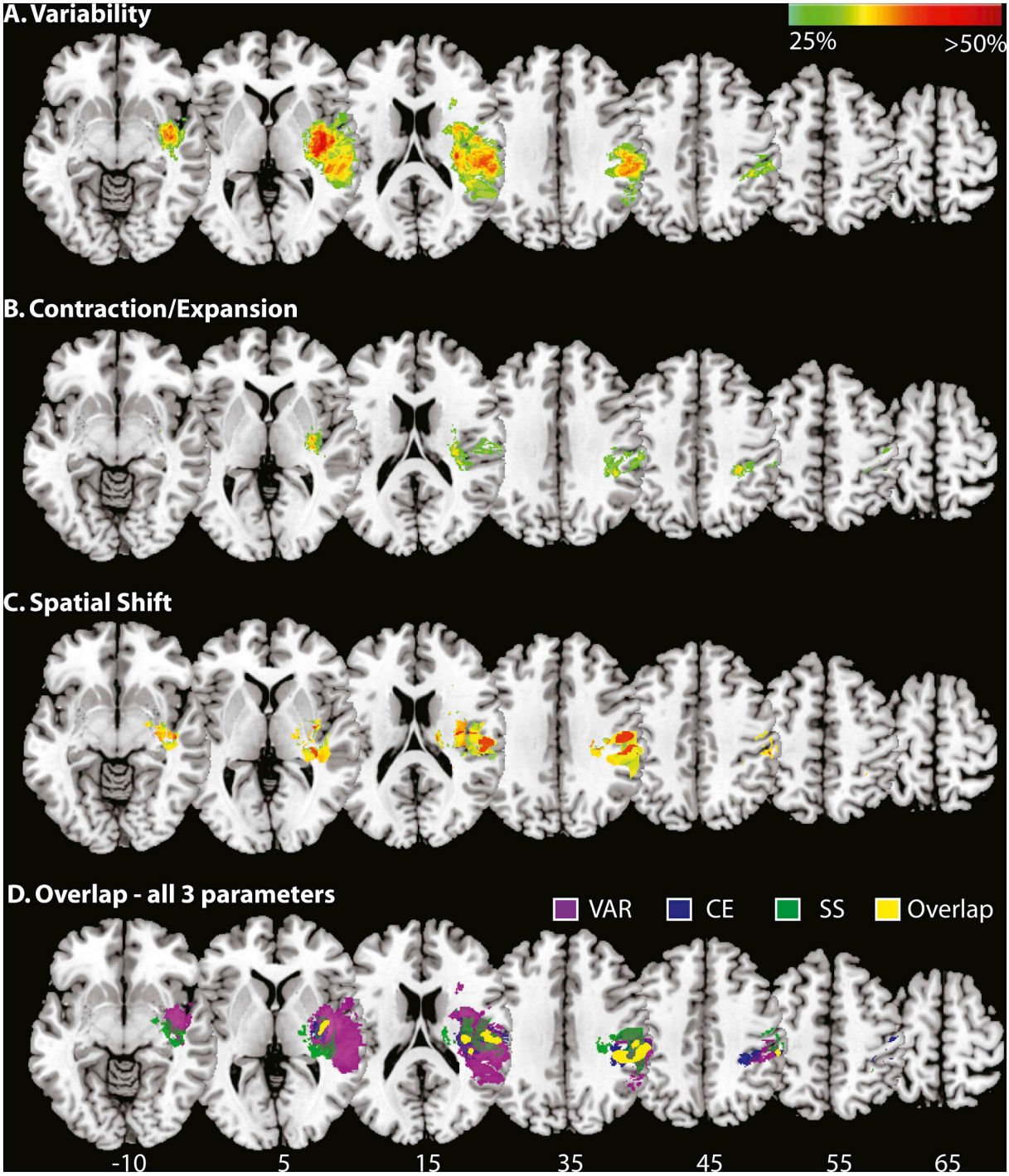

Fig. 6. Lesion frequency analysis for the position matching parameters.
A) Variability B) Contraction/Expansion C) Spatial shift. Colour bar indicates the regions where damage is more frequently seen in subjects with deficits than in subjects without deficits. Only regions where the frequency is > 20% are shown. In panel D the above maps are superimposed and regions where all 3 parameters overlap are in yellow. Abbreviations VAR, Variability; CE, Contraction/Expansion; SS, Spatial Shift.

localization has been attributed to this region (Altmann et al., 2007; Baumgart et al., 1999; Zatorre and Penhune, 2001) and it is connected with the frontoparietal network (Shinn et al., 2013). Our findings suggest that circuitry involved in propriospatial localization involves Heschl's gyrus and extends its role beyond auditory spatial localization.

Importantly, damage to the corticospinal tract (CST) was associated with poor performance on the contraction/expansion, peak speed ratio, and initial direction error parameters at the final timepoint. The CST is known to originate from a number of cortical areas, including the primary somatosensory cortex, the posterior parietal cortex, and the parietal operculum in monkeys (Lemon and Griffiths, 2005) and play a role in controlling ascending sensory information as it enters the spinal cord (Canedo, 1997). Thus, the CST is considered by some to be more than just a motor tract (Lemon and Griffiths, 2005) which may account for its association with abnormal proprioceptive performance in our study.

Taken together, these findings suggest that a distributed cortical and sub-cortical network is required to perceive proprioceptive information.

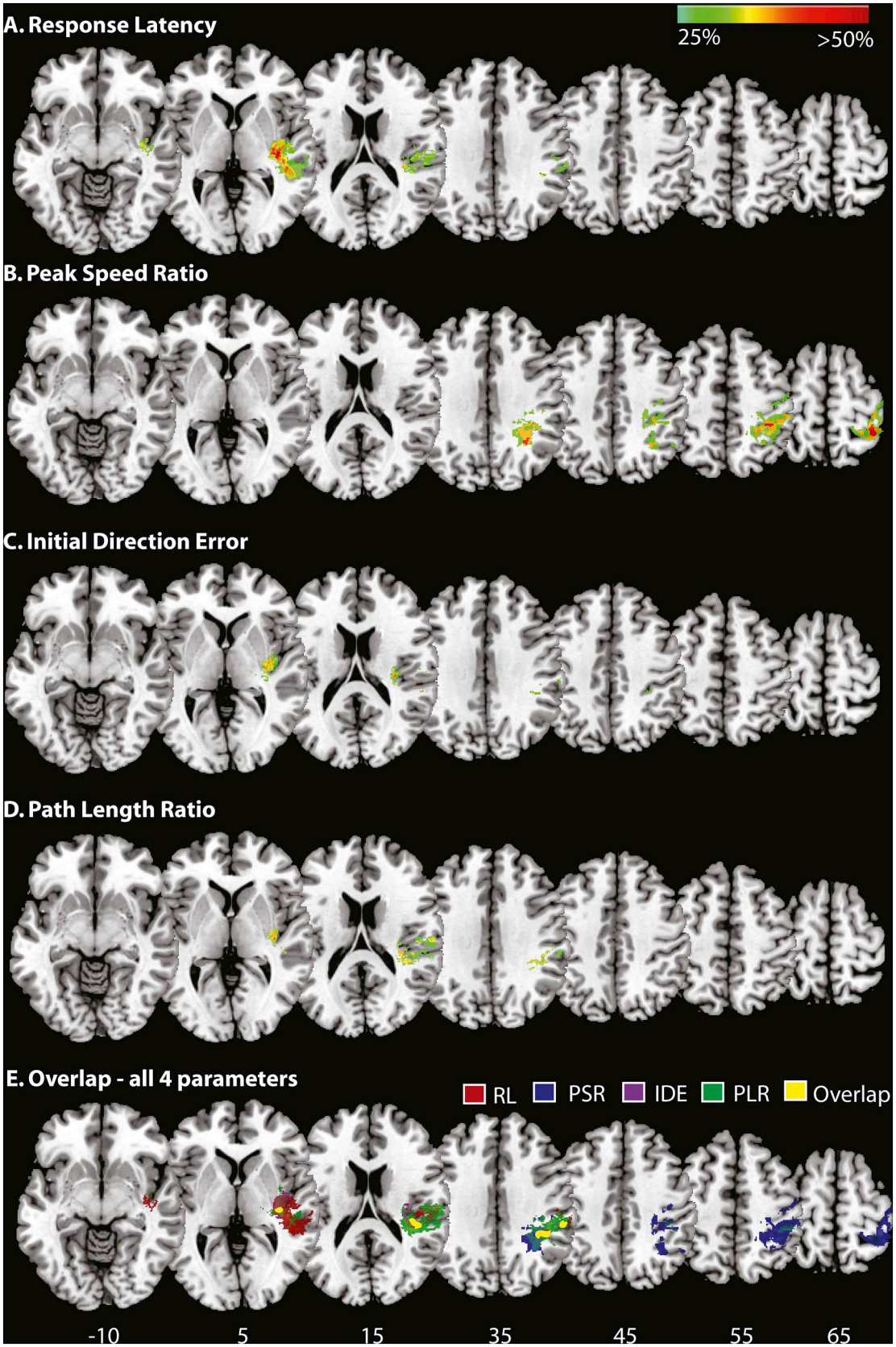

Fig. 7. Lesion frequency analysis for the kinesthetic matching parameters.
A) Response Latency B) Peak Speed Ratio C) Initial Direction Error D) Path Length Ratio. Colour bar indicates the regions where damage is more frequently seen in subjects with deficits than in subjects without deficits. Only regions where the frequency is > 20% are shown. In panel E the above maps are superimposed and regions where all 4 parameters overlap are circled in yellow. Abbreviations: RL, Response Latency; PSR, Peak Speed Ratio; IDE, Initial Direction Error; PLR, Path Length Ratio.

We included individuals with brainstem and cerebellar stroke in the present study as these patients often present on stroke rehabilitation units with proprioceptive deficits. We are not aware of previous studies outside of our own (Semrau et al., 2015) that attempt to document proprioceptive recovery in these types of lesions. Anecdotally, with increased use of thrombolysis and mechanical embolectomy on acute stroke units for typical Middle Cerebral Artery (MCA) strokes, the relative number of patients with brainstem and cerebellar stroke lesions on our local rehabilitation units seems to be increasing, thus making this an important area for future research.

4.1. Limitations

There is much interest in hemispheric lateralization of functions. For our current study in proprioceptive recovery, this was difficult to address as our inclusion criteria necessitated that subjects have sufficient language function to understand the tasks, resulting in the exclusion of subjects with large left hemisphere lesions. Despite this, we had a large number of individuals with both right and left brain lesions who had problems with proprioception. However, excluding individuals with large left hemisphere lesions creates challenges in making conclusions about hemispheric differences in proprioception. Similarly, our study had too few subjects with cerebellar or brainstem lesions to make firm conclusions about recovery in these groups. Future studies with larger sample sizes are required to examine proprioception in subjects with brainstem and cerebellar lesions.

Combining CT and MRI for lesion studies may be controversial. However, we agree with Sperber and Karnath (2016) who argue that many major stroke centres use CT's due to cost and timeliness. Excluding subjects with only CT scans may result in a sampling bias and creates unnecessary expense. Further, viewer enhancements make marking CT's easier and modern registration tools provide very accurate results.

Finally, the majority of subjects in our sample had mild or moderate stroke severity. Subjects with more severe stroke tend to be too unwell to participate in the first time point for our study. This may affect the generalizability of our results in individuals with severe strokes, but it is likely that many of these individuals experience proprioceptive impairments with the same prevalence, or potentially higher than our present sample.

5. Conclusion

Our findings that lesions in the supramarginal gyrus, arcuate fasciculus, and Heschl's gyrus are associated with poor proprioceptive recovery extends our understanding of brain regions associated with proprioception. Further, we observed that proprioceptive impairment is common and persistent after stroke, particularly in the cortical and subcortical lesions. This leads us to question whether proprioceptive deficits are effectively targeted in rehabilitation – and if they are not, would doing so decrease the incidence of impairments? These findings may inform personalized interventions such as non-invasive brain stimulation where specific regions of the brain can be targeted to potentially alter stroke recovery trajectories.

Supplementary data to this article can be found online at https://doi.org/10.1016/j.nicl.2018.10.003.

Funding sources

The present work was supported by a Canadian Institutes of Health Research Grant (MOP 106662), a Heart and Stroke Foundation of Canada Grant-in-Aid (G-13-003029), an Alberta Innovates Health Solutions Team Grant (201500788), and an Ontario Research Fund Grant (ORF-RE 04-47). SEF was supported by an Alberta Innovates Health Solutions Clinical Fellowship.

Acknowledgments

The authors wish to thank Ms. Janice Yajure and Mr. Mark Piitz for their assistance with subject recruitment and assessment.

References

Abela, E., Missimer, J., Wiest, R., Federspiel, A., Hess, C., Sturzenegger, M., Weder, B., 2012. Lesions to primary sensory and posterior parietal cortices impair recovery from hand paresis after stroke. PLoS One 7 (2), e31275. https://doi.org/10.1371/journal.pone.0031275.

Academy of Neurologic Physical Therapy. (2011). StrokeEDGE Documents. Retrieved from http://www.neuropt.org/professional-resources/neurology-section-outcome-measuresrecommendations/stroke:

Altmann, C.F., Bledowski, C., Wibral, M., Kaiser, J., 2007. Processing of location and pattern changes of natural sounds in the human auditory cortex. NeuroImage 35 (3), 1192–1200. https://doi.org/10.1016/j.neuroimage.2007.01.007.

Amaral, D., 2013. The functional organization of perception and movement. In: Kandell, E., Schwartz, J., Jessell, T., Siegelbaum, S., Hudspeth, A. (Eds.), Principles of Neural Science. McGraw-Hill, New York, pp. 356–369 5 ed.

Baumgart, F., Gaschler-Markefski, B., Woldorff, M.G., Heinze, H.J., Scheich, H., 1999. A movement-sensitive area in auditory cortex. Nature 400 (6746), 724–726. https://doi.org/10.1038/23385.

Ben-Shabat, E., Matyas, T.A., Pell, G.S., Brodtmann, A., Carey, L.M., 2015. The right supramarginal Gyrus is Important for proprioception in healthy and stroke-affected participants: a functional MRI study. Front. Neurol. 6, 248. https://doi.org/10.3389/fneur.2015.00248.

Bohannon, R.W., Smith, M.B., 1987. Interrater reliability of a modified Ashworth scale of muscle spasticity. Phys. Ther. 67 (2), 206–207.

Brett, M., Leff, A.P., Rorden, C., Ashburner, J., 2001. Spatial normalization of brain images with focal lesions using cost function masking. NeuroImage 14 (2), 486–500. https://doi.org/10.1006/nimg.2001.0845.

Brozzoli, C., Gentile, G., Petkova, V.I., Ehrsson, H.H., 2011. FMRI adaptation reveals a cortical mechanism for the coding of space near the hand. J. Neurosci. 31 (24), 9023–9031. https://doi.org/10.1523/JNEUROSCI.1172-11.2011.

Canedo, A., 1997. PRIMARY MOTOR CORTEX INFLUENCES ON THE DESCENDING AND ASCENDING SYSTEMS. Prog. Neurobiol. 51 (3), 287–335. https://doi.org/10.1016/S0301-0082(96)00058-5.

Carey, L.M., Matyas, T.A., 2011. Frequency of discriminative sensory loss in the hand after stroke in a rehabilitation setting. J. Rehabil. Med. 43 (3), 257–263. https://doi.org/10.2340/16501977-0662.

Cassidy, A., 2016. The clinical assessment of apraxia. Pract. Neurol. 16 (4), 317–322. https://doi.org/10.1136/practneurol-2015-001354.

Catani, M., Thiebaut de Schotten, M., 2008. A diffusion tensor imaging tractography atlas for virtual in vivo dissections. Cortex 44 (8), 1105–1132. https://doi.org/10.1016/j.cortex.2008.05.004.

Catani, M., Jones, D.K., Ffytche, D.H., 2005. Perisylvian language networks of the human brain. Ann. Neurol. 57 (1), 8–16. https://doi.org/10.1002/ana.20319.

Chen, C.L., Tang, F.T., Chen, H.C., Chung, C.Y., Wong, M.K., 2000. Brain lesion size and location: effects on motor recovery and functional outcome in stroke patients. Arch. Phys. Med. Rehabil. 81 (4), 447–452. https://doi.org/10.1053/mr.2000.3837.

Coderre, A.M., Zeid, A.A., Dukelow, S.P., Demmer, M.J., Moore, K.D., Demers, M.J., Scott, S.H., 2010. Assessment of upper-limb sensorimotor function of subacute stroke patients using visually guided reaching. Neurorehabil. Neural Repair 24 (6), 528–541. https://doi.org/10.1177/1545968309356091.

Connell, L.A., Lincoln, N.B., Radford, K.A., 2008. Somatosensory impairment after stroke: frequency of different deficits and their recovery. Clin. Rehabil. 22 (8), 758–767. https://doi.org/10.1177/0269215508090674.

Dick, A.S., Tremblay, P., 2012. Beyond the arcuate fasciculus: consensus and controversy in the connectional anatomy of language. Brain 135, 3529–3550. https://doi.org/10.1093/brain/aws222. Pt 12.

Doughty, C., Wang, J., Feng, W., Hackney, D., Pani, E., Schlaug, G., 2016. Detection and Predictive Value of Fractional Anisotropy changes of the Corticospinal Tract in the Acute phase of a Stroke. Stroke 47 (6), 1520–1526. https://doi.org/10.1161/STROKEAHA.115.012088.

Dukelow, S.P., Herter, T.M., Moore, K.D., Demers, M.J., Glasgow, J.I., Bagg, S.D., Scott, S.H., 2010. Quantitative assessment of limb position sense following stroke. Neurorehabil. Neural Repair 24 (2), 178–187. https://doi.org/10.1177/1545968309345267.

Dukelow, S.P., Herter, T.M., Bagg, S.D., Scott, S.H., 2012. The independence of deficits in position sense and visually guided reaching following stroke. Journal of Neuroengineering and Rehabilitation 9, 72. https://doi.org/10.1186/1743-0003-9-72.

Felton, D.L., Shetty, A.N., 2010. Netter's Atlas of Neuroscience. 2nd Edition ed.. Sauders Elsevier, Philadelphia, PA.

Feng, W., Wang, J., Chhatbar, P.Y., Doughty, C., Landsittel, D., Lioutas, V.A., Schlaug, G., 2015. Corticospinal tract lesion load: an imaging biomarker for stroke motor outcomes. Ann. Neurol. 78 (6), 860–870. https://doi.org/10.1002/ana.24510.

Findlater, S.E., Desai, J.A., Semrau, J.A., Kenzie, J.M., Rorden, C., Herter, T.M., Dukelow, S.P., 2016. Central perception of position sense involves a distributed neural network - evidence from lesion-behavior analyses. Cortex 79 (79), 42–56. https://doi.org/10.1016/j.cortex.2016.03.008.

Friston, K.J., Holmes, A.P., Worsley, K.J., Poline, J.P., Frith, C.D., Frackowiak, R.S.J., 1994. Statistical parametric maps in functional imaging: a general linear approach.

Hum. Brain Mapp. 2 (4), 189–210. https://doi.org/10.1002/hbm.460020402.
Gardner, E., Johnson, K., 2013. The Somaotosensory System: Receptors and Central Pathways. In: Kandell, E., Schwartz, J., Jessell, T., Siegelbaum, S., Hudspeth, A. (Eds.), Principles of Neural Science. McGraw-Hill, New York, pp. 473–497.
Globas, C., Lam, J.M., Zhang, W., Imanbayev, A., Hertler, B., Becker, C., Luft, A.R., 2011. Mesencephalic corticospinal atrophy predicts baseline deficit but not response to unilateral or bilateral arm training in chronic stroke. Neurorehabil. Neural Repair 25 (1), 81–87. https://doi.org/10.1177/1545968310382001.
Goble, D.J., Brown, S.H., 2009. Dynamic proprioceptive target matching behavior in the upper limb: effects of speed, task difficulty and arm/hemisphere asymmetries. Behav. Brain Res. 200 (1), 7–14. https://doi.org/10.1016/j.bbr.2008.11.034.
Goble, D.J., Lewis, C.A., Brown, S.H., 2006. Upper limb asymmetries in the utilization of proprioceptive feedback. Exp. Brain Res. 168 (1–2), 307–311. https://doi.org/10.1007/s00221-005-0280-y.
Goldenberg, G., Karnath, H.O., 2006. The neural basis of imitation is body part specific. J. Neurosci. 26 (23), 6282–6287. https://doi.org/10.1523/jneurosci.0638-06.2006.
Gowland, C., Stratford, P., Ward, M., Moreland, J., Torresin, W., Van Hullenaar, S., Plews, N., 1993. Measuring physical impairment and disability with the Chedoke-McMaster Stroke Assessment. Stroke 24 (1), 58–63. https://doi.org/10.1161/01.str.24.1.58.
de Haan, B., Karnath, H.O., 2017. A hitchhiker's guide to lesion-behaviour mapping. Neuropsychologia. https://doi.org/10.1016/j.neuropsychologia.2017.10.021.
Hawe, R.L., Findlater, S.E., Kenzie, J.M., Hill, M.D., Scott, S.H., Dukelow, S., 2018. Differential Impact of Acute Lesions Versus White Matter Hyperintensities on Stroke Recovery. J. Am. Heart Assoc. 7 (18), 1–14. https://doi.org/10.1161/JAHA.118.009360.
Herter, T.M., 2011. Technical Document: Normative Data Modeling - Position Matching Task.
van Heugten, C.M., Dekker, J., Deelman, B.G., Stehmann-Saris, F.C., Kinebanian, A., 1999. A diagnostic test for apraxia in stroke patients: internal consistency and diagnostic value. Clin. Neuropsychol. 13 (2), 182–192. https://doi.org/10.1076/clin.13.2.182.1966.
Hirayama, K., Fukutake, T., Kawamura, M., 1999. "Thumb localizing test" for detecting a lesion in the posterior column-medial lemniscal system. J. Neurol. Sci. 1999 (167), 45–49.
Iwamura, Y., 2003. Somatosensory Association Cortices. (Paper presented at the International Congress Series).
Karnath, H.O., Rennig, J., 2017. Investigating structure and function in the healthy human brain: validity of acute versus chronic lesion-symptom mapping. Brain Struct. Funct. 222 (5), 2059–2070. https://doi.org/10.1007/s00429-016-1325-7.
Karnath, H.O., Himmelbach, M., Rorden, C., 2002. The subcortical anatomy of human spatial neglect: putamen, caudate nucleus and pulivar. Brain 125, 350–360.
Karnath, H.O., Rorden, C., Ticini, L.F., 2009. Damage to white matter fiber tracts in acute spatial neglect. Cereb. Cortex 19 (10), 2331–2337. https://doi.org/10.1093/cercor/bhn250.
Karnath, H.O., Rennig, J., Johannsen, L., Rorden, C., 2011. The anatomy underlying acute versus chronic spatial neglect: a longitudinal study. Brain 134, 903–912. https://doi.org/10.1093/brain/awq355. Pt 3.
Keith, R.A., Granger, C.V., Hamilton, B.B., Sherwin, F.S., 1987. The functional independence measure: a new tool for rehabilitation. Adv. Clin. Rehabil. 1, 6–18.
Kenzie, J.M., Semrau, J.A., Findlater, S.E., Yu, A.Y., Desai, J.A., Herter, T.M., Dukelow, S.P., 2016. Localization of Impaired Kinesthetic Processing Post-stroke. Front. Hum. Neurosci. 10, 505. https://doi.org/10.3389/fnhum.2016.00505.
Kenzie, J.M., Semrau, J.A., Hill, M.D., Scott, S.H., Dukelow, S.P., 2017. A composite robotic-based measure of upper limb proprioception. Journal of Neuroengineering and Rehabilitation 14 (1), 114. https://doi.org/10.1186/s12984-017-0329-8.
Kim, N.Y., Lee, S.C., Shin, J.C., Park, J.E., Kim, Y.W., 2017. Voxel-based lesion symptom mapping analysis of depressive mood in patients with isolated cerebellar stroke: a pilot study. Neuroimage Clin 13, 39–45. https://doi.org/10.1016/j.nicl.2016.11.011.
Kuper, M., Hermsdorfer, J., Brandauer, B., Thurling, M., Schoch, B., Theysohn, N., Timmann, D., 2011. Lesions of the dentate and interposed nuclei are associated with impaired prehension in cerebellar patients. Neurosci. Lett. 499 (2), 132–136. https://doi.org/10.1016/j.neulet.2011.05.055.
Leiguarda, R.C., Marsden, C.D., 2000. Limb apraxias: higher-order disorders of sensorimotor integration. Brain (123), 860–879 Pt 5.
Lemon, R.N., Griffiths, J., 2005. Comparing the function of the corticospinal system in different species: organizational differences for motor specialization? Muscle ad Nerve 32 (3), 261–279. https://doi.org/10.1002/mus.20333.
Lincoln, N.B., Crow, J.L., Jackson, J.M., Waters, G.R., Adams, S.A., Hodgson, P., 1991. The unreliability of sensory assessments. Clin. Rehabil. 5 (4), 273–282. https://doi.org/10.1177/026921559100500403.
Lincoln, N.B., Jackson, J.M., Adams, S.A., 1998. Reliability and Revision of the Nottingham Sensory Assessment for Stroke patients. Physiotherapy 84 (8), 358–365. https://doi.org/10.1016/s0031-9406(05)61454-x.
Lisberger, S., Thach, W., 2012. The Cerebellum. In: Kandell, E., Schwartz, J., Jessell, T., Siegelbaum, S., Hudspeth, A. (Eds.), Principles of Neural Science. McGraw-Hill, New York, pp. 960–981 5 ed.
Lo, R., Gitelman, D., Levy, R., Hulvershorn, J., Parrish, T., 2010. Identification of critical areas for motor function recovery in chronic stroke subjects using voxel-based lesion symptom mapping. NeuroImage 49 (1), 9–18. https://doi.org/10.1016/j.neuroimage.2009.08.044.
Löuvbld, K.-O., Baird, A.E., Schlaug, G., Benfield, A., Siewert, B., Voetsch, B., Warach, S., 1997. Ischemic lesion volumes in acute stroke by diffusion-weighted magnetic resonance imaging correlate with clinical outcome. Ann. Neurol. 42 (2), 164–170. https://doi.org/10.1002/ana.410420206.
Lunven, M., Thiebaut De Schotten, M., Bourlon, C., Duret, C., Migliaccio, R., Rode, G., Bartolomeo, P., 2015. White matter lesional predictors of chronic visual neglect: a longitudinal study. Brain 138, 746–760. https://doi.org/10.1093/brain/awu389. Pt 3.
McCloskey, D., 1973. Differences between the senses of movement and position shown by the effects of loading and vibration of muscles in man. Brain Res. 63, 119–131.
Meyer, S., De Bruyn, N., Krumlinde-Sundholm, L., Peeters, A., Feys, H., Thijs, V., Verheyden, G., 2016a. Associations between Sensorimotor Impairments in the Upper Limb at 1 Week and 6 months after Stroke. J. Neurol. Phys. Ther. 40 (3), 186–195. https://doi.org/10.1097/NPT.0000000000000138.
Meyer, S., Kessner, S.S., Cheng, B., Bonstrup, M., Schulz, R., Hummel, F.C., Verheyden, G., 2016b. Voxel-based lesion-symptom mapping of stroke lesions underlying somatosensory deficits. Neuroimage Clin 10, 257–266. https://doi.org/10.1016/j.nicl.2015.12.005.
Naito, E., Roland, P.E., Grefkes, C., Choi, H.J., Eickhoff, S., Geyer, S., Ehrsson, H.H., 2005. Dominance of the right hemisphere and role of area 2 in human kinesthesia. J. Neurophysiol. 93 (2), 1020–1034. https://doi.org/10.1152/jn.00637.2004.
Naito, E., Nakashima, T., Kito, T., Aramaki, Y., Okada, T., Sadato, N., 2007. Human limb-specific and non-limb-specific brain representations during kinesthetic illusory movements of the upper and lower extremities. Eur. J. Neurosci. 25 (11), 3476–3487. https://doi.org/10.1111/j.1460-9568.2007.05587.x.
Naito, E., Morita, T., Saito, D.N., Ban, M., Shimada, K., Okamoto, Y., Asada, M., 2017. Development of Right-hemispheric Dominance of Inferior Parietal Lobule in Proprioceptive Illusion Task. Cereb. Cortex 27 (11), 5385–5397. https://doi.org/10.1093/cercor/bhx223.
Oldfield, R.C., 1971. The assessment and analysis of handedness: the Edinburgh inventory. Neuropsychologia 9 (1), 97–113. https://doi.org/10.1016/0028-3932(71)90067-4.
Oscarsson, O., Uddenberg, N., 1964. Identification of a Spinocerebellar Tract Activated from Forelimb Afferents in the Cat. Acta Physiol. Scand. 62, 125–136. https://doi.org/10.1111/j.1748-1716.1964.tb03960.x.
Ovadia-Caro, S., Villringer, K., Fiebach, J., Jungehulsing, G.J., van der Meer, E., Margulies, D.S., Villringer, A., 2013. Longitudinal effects of lesions on functional networks after stroke. J. Cereb. Blood Flow Metab. 33 (8), 1279–1285. https://doi.org/10.1038/jcbfm.2013.80.
Pandya, D.N., Seltzer, B., 1982. Association areas of the cerebral cortex. Trends Neurosci. 5, 386–390.
Pearson, K., Gordon, J., 2013. Spinal Reflexes. In: Kandell, E., Schwartz, J., Jessell, T., Siegelbaum, S., Hudspeth, A. (Eds.), Principles of Neural Science. McGraw-Hill, New York, pp. 790–811 5 ed.
Puig, J., Pedraza, S., Blasco, G., Daunis, I.E.J., Prats, A., Prados, F., Serena, J., 2010. Wallerian degeneration in the corticospinal tract evaluated by diffusion tensor imaging correlates with motor deficit 30 days after middle cerebral artery ischemic stroke. AJNR Am. J. Neuroradiol. 31 (7), 1324–1330. https://doi.org/10.3174/ajnr.A2038.
Purves, D., Augustine, G., Fitzpatrick, D., Hall, W., LaMantia, A., McNamara, J., White, L. (Eds.), 2008. Neuroscience, Fourth Edition ed. Sinauer Associates, Inc, Sunderland, Massachusetts.
Rorden, C., Karnath, H.O., Bonilha, L., 2007. Improving lesion-symptom mapping. J. Cogn. Neurosci. 19 (7), 1081–1088. https://doi.org/10.1162/jocn.2007.19.7.1081.
Rorden, C., Bonilha, L., Fridriksson, J., Bender, B., Karnath, H.O., 2012. Age-specific CT and MRI templates for spatial normalization. NeuroImage 61 (4), 957–965. https://doi.org/10.1016/j.neuroimage.2012.03.020.
Saunders, D.E., Clifton, A.G., Brown, M.M., 1995. Measurement of infarct size using MRI predicts prognosis in middle cerebral artery infarction. Stroke 26 (12), 2272–2276.
Semrau, J.A., Herter, T.M., Scott, S.H., Dukelow, S.P., 2013a. Comparison of post-stroke position sense and kinaesthia using robotics. In: Paper presented at the Society for Neuroscience, San Diego, CA.
Semrau, J.A., Herter, T.M., Scott, S.H., Dukelow, S.P., 2013b. Robotic identification of kinesthetic deficits after stroke. Stroke 44 (12), 3414–3421. https://doi.org/10.1161/STROKEAHA.113.002058.
Semrau, J.A., Herter, T.M., Scott, S.H., Dukelow, S.P., 2015. Examining differences in patterns of Sensory and Motor Recovery after Stroke with Robotics. Stroke 46 (12), 3459–3469. https://doi.org/10.1161/STROKEAHA.115.010750.
Semrau, J.A., Herter, T.M., Kenzie, J.M., Findlater, S.E., Scott, S.H., Dukelow, S.P., 2017. Robotic Characterization of Ipsilesional Motor Function in Subacute Stroke. Neurorehabil. Neural Repair 31 (6), 571–582. https://doi.org/10.1177/1545968317704903.
Shinn, A.K., Baker, J.T., Cohen, B.M., Ongur, D., 2013. Functional connectivity of left Heschl's gyrus in vulnerability to auditory hallucinations in schizophrenia. Schizophr. Res. 143 (2–3), 260–268. https://doi.org/10.1016/j.schres.2012.11.037.
Sherrington, C., 1907. On the proprioceptive system, especially in its reflex aspect. Brain 29, 467–482.
Simmatis, L., Krett, J., Scott, S.H., Jin, A.Y., 2017. Robotic exoskeleton assessment of transient ischemic attack. PLoS One 12 (12).
Sperber, C., Karnath, H.O., 2016. Topography of acute stroke in a sample of 439 right brain damaged patients. Neuroimage Clin 10, 124–128. https://doi.org/10.1016/j.nicl.2015.11.012.
Sperber, C., Karnath, H.-O., 2018. On the validity of lesion-behaviour mapping methods. Neuropsychologia 115, 17–24. https://doi.org/10.1016/j.neuropsychologia.2017.07.035.
BKIN Technologies, 2016. Dexterit-E 3.6 User Guide. Kingston, ON.
Thiebaut De Schotten, M., Dell'Acqua, F., Forkel, S.J., Simmons, A., Vergani, F., Murphy, D.G., Catani, M., 2011. A lateralized brain network for visuospatial attention. Nat. Neurosci. 14 (10), 1245–1246. https://doi.org/10.1038/nn.2905.
Thomalla, G., Glauche, V., Weiller, C., Rother, J., 2005. Time course of wallerian degeneration after ischaemic stroke revealed by diffusion tensor imaging. Journal of Neurology. Neurosurgery and Psychiatry 76 (2), 266–268. https://doi.org/10.1136/

jnnp.2004.046375.
Tzourio-Mazoyer, N., Landeau, B., Papathanassiou, D., Crivello, F., Etard, O., Delcroix, N., Joliot, M., 2002. Automated anatomical labeling of activations in SPM using a macroscopic anatomical parcellation of the MNI MRI single-subject brain. NeuroImage 15 (1), 273–289. https://doi.org/10.1006/nimg.2001.0978.
Verdon, V., Schwartz, S., Lovblad, K.O., Hauert, C.A., Vuilleumier, P., 2010. Neuroanatomy of hemispatial neglect and its functional components: a study using voxel-based lesion-symptom mapping. Brain 133 (Pt 3), 880–894. https://doi.org/10.1093/brain/awp305.
Vidoni, E.D., Boyd, L.A., 2009. Preserved motor learning after stroke is related to the degree of proprioceptive deficit. Behav. Brain Funct. 5, 36. https://doi.org/10.1186/1744-9081-5-36.
Wasserthal, C., Brechmann, A., Stadler, J., Fischl, B., Engel, K., 2014. Localizing the human primary auditory cortex in vivo using structural MRI. Neuroimage 93 Pt 2 (0), 237–251. https://doi.org/10.1016/j.neuroimage.2013.07.046.
Weiller, C., Juptner, M., Fellows, S., Rijntjes, M., Leonhardt, G., Kiebel, S., Thilmann, A.F., 1996. Brain representation of active and passive movements. NeuroImage 4 (2), 105–110. https://doi.org/10.1006/nimg.1996.0034.
Wilson, B., Cockburn, J., Halligan, P., 1988. Behavioural inattention test. Thames Valley Test Company, Fareham, UK.
Winder, K., Seifert, F., Ohnemus, T., Sauer, E.M., Kloska, S., Dörfler, A., Köhrmann, M., 2015. Neuroanatomic correlates of poststroke hyperglycemia. Ann. Neurol. 77 (2), 262–268. https://doi.org/10.1002/ana.24322.
Winward, C.E., Halligan, P.W., Wade, D.T., 2002. The Rivermead Assessment of Somatosensory Performance (RASP): standardization and reliability data. Clin. Rehabil. 16 (5), 523–533. https://doi.org/10.1191/0269215502cr522oa.
Winward, C.E., Halligan, P.W., Wade, D.T., 2007. Somatosensory recovery: a longitudinal study of the first 6 months after unilateral stroke. Disabil. Rehabil. 29 (4), 293–299. https://doi.org/10.1080/09638280600756489.
Wu, O., Cloonan, L., Mocking, S.J., Bouts, M.J., Copen, W.A., Cougo-Pinto, P.T., ... Rost, N.S., 2015. Role of acute lesion topography in initial ischemic stroke severity and long-term functional outcomes. Stroke 46 (9), 2438–2444. https://doi.org/10.1161/strokeaha.115.009643.
Zatorre, R.J., Penhune, V.B., 2001. Spatial localization after excision of human auditory cortex. J. Neurosci. 21 (16), 6321–6328.
Zhu, L.L., Lindenberg, R., Alexander, M.P., Schlaug, G., 2010. Lesion load of the corticospinal tract predicts motor impairment in chronic stroke. Stroke 41 (5), 910–915. https://doi.org/10.1161/STROKEAHA.109.577023.